Anomalous anisotropic exciton temperature dependence in rutile TiO₂

Edoardo Baldini,[1,*] Adriel Dominguez,[2] Letizia Chiodo,[3] Evgeniia Sheveleva,[4] Meghdad Yazdi-Rizi,[4]
Christian Bernhard,[4] Angel Rubio,[2,5] and Majed Chergui[1]

[1]*Laboratory of Ultrafast Spectroscopy, ISIC and Lausanne Centre for Ultrafast Science (LACUS), École Polytechnique Fédérale de Lausanne, CH-1015 Lausanne, Switzerland*
[2]*Max Planck Institute for the Structure and Dynamics of Matter, D-22761 Hamburg, Germany*
[3]*Unit of Nonlinear Physics and Mathematical Modeling, Department of Engineering, Università Campus Bio-Medico di Roma, Via Álvaro del Portillo 21, I-00128, Rome, Italy*
[4]*Department of Physics, University of Fribourg, Chemin du Musée 3, CH-1700 Fribourg, Switzerland*
[5]*Departamento Física de Materiales, Universidad del País Vasco, Avenida Tolosa 72, E-20018 San Sebastián, Spain*

Elucidating the details of electron-phonon coupling in semiconductors and insulators is a topic of pivotal interest, as it governs the transport mechanisms and is responsible for various phenomena such as spectral-weight transfers to phonon sidebands and self-trapping. Here, we investigate the influence of the electron-phonon interaction on the excitonic peaks of rutile TiO₂, revealing a strong anisotropic polarization dependence with increasing temperature, namely, an anomalous blue shift for light polarized along the *a* axis and a conventional red shift for light polarized along the *c* axis. By employing many-body perturbation theory, we identify two terms in the electron-phonon interaction Hamiltonian that contribute to the anomalous blue shift of the *a*-axis exciton. Our approach paves the way to a complete *ab initio* treatment of the electron-phonon interaction and of its influence on the optical spectra of polar materials.

The temperature (T) dependence of elementary excitations is a central subject in condensed matter physics, as it provides insightful information on the microscopic details of many-body interactions and correlations. To this end, over the past five decades, considerable efforts have been devoted to studying T effects on the optical spectra of materials, where elementary excitations in the long-wavelength regime possess a clear spectroscopic fingerprint. In this regard, an old topic is represented by the T dependence of interband transitions and excitons in standard band semiconductors and insulators [1,2]. The energy of these excitations (E_{exc}) typically undergoes a sizable softening with increasing T, but in a few exceptional cases, the opposite effect or more complex T dependences have been observed [3–5]. Part of this renormalization is accounted for by the thermal expansion of the lattice, but the major contribution arises from the structure of the electron-phonon interaction (EPI).

To model the measured dependences of E_{exc}, simple algebraic expressions were initially used, the most common of which is the empirical Varshni law [6]. More accurate fits were obtained by using Bose-Einstein statistical factors with average acoustic and optical phonon frequencies, an approach that finds theoretical justification in pseudopotential theory [7]. Within this framework, anomalous T dependences of E_{exc} can be described by assuming that the contributions due to phonons with low and high frequencies retain opposite signs [8]. A more rigorous generalization of this approach, using a distribution of phonon energies, was proposed [9], in which $E_{exc}(T)$ can be described as

$$E_{exc}(T) = E_0 - \int d\omega f(\omega)\left[n_{BE}(\omega,T) + \frac{1}{2}\right] - E_{th}(T),$$

(1)

where E_0 is the energy gap at zero T, n_{BE} is the Bose-Einstein statistical factor ($(e^{\hbar\omega/k_BT} - 1)^{-1}$, $f(\omega)$ is a weighting factor, and the last term $E_{th}(T)$ accounts for the lattice thermal expansion. The weighting factor $f(\omega)$ can be decomposed into a product of the phonon density of states (PDOS) and a factor related to the EPI strength. However, this method suffers from intrinsic complexity, requiring detailed knowledge of the measured/calculated PDOS and EPI constants. Approximated models have been employed in isotropic materials, where the PDOS is characterized by van Hove singularities associated with specific phonon modes [10]. In summary, the strength of these models lies in their ability to reveal the coarse features of the EPI, albeit at a phenomenological level. As a result, these methods lose track of the microscopic details of the EPI, for which a full *ab initio* treatment is needed. A step further in this respect involves the description of different sources contributing to the EPI in materials with an intrinsic degree of optical anisotropy.

In this paper, we perform T-dependent spectroscopic ellipsometry (SE) measurements on the polar insulator rutile TiO₂. To our knowledge, this is the first study to report the low-T spectra of this material and it reveals an anomalous anisotropic T dependence of its resonant excitons. By applying state-of-the-art many-body perturbation theory calculations, we go beyond the established phenomenological models, identifying two terms in the EPI Hamiltonian which lead to the exciton hardening with increasing T. Our study paves the way to a complete quantitative treatment of the EPI in strongly interacting semiconductors and insulators. This aspect becomes of special interest for improving the design of future electrical and optoelectronic devices, in which the interaction between electrons and phonons can affect the carrier mobility or lead to the emergence of polaronic species.

The SE measurements were performed on a (010)-oriented rutile TiO₂ single crystal. SE provides significant advantages
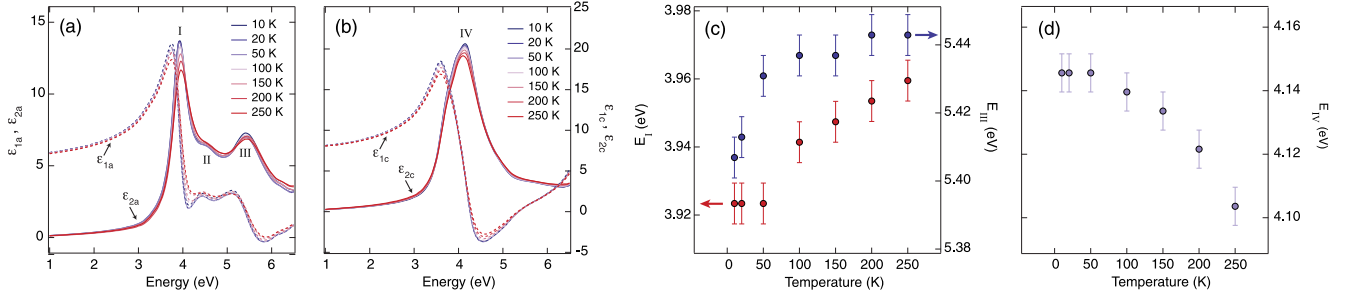
*edoardo.baldini@epfl.ch

FIG. 1. Measured T dependence of the dielectric function of a rutile TiO_2 single crystal in (a) a-axis and (b) c-axis polarization. Behavior of the peak energy for (c) charge excitations I and III and (d) charge excitation IV as a function of T.

over conventional reflection methods: (i) it is self-normalizing and does not require reference measurements; (ii) $\epsilon_1(\omega)$ and $\epsilon_2(\omega)$ are obtained directly, without a Kramers-Kronig transformation; and (iii) in the ultraviolet, SE is less affected by the surface roughness of the sample than normal-incidence reflectivity. Many-body perturbation theory at the level of the GW and the Bethe-Salpeter equation (BSE) [11,12] was employed to compute the band structure and the dielectric response of rutile TiO_2. Details of the experimental methods and the *ab initio* calculations are reported in the Supplemental Material (SM) [13].

Figures 1(a) and 1(b) show the spectra of the real and imaginary parts of the dielectric function, $\epsilon_1(\omega)$ and $\epsilon_2(\omega)$, along the a and c axis, respectively, at different T's. As expected, the substantial difference between the lattice constants, $a = 4.59\,\text{Å}$ and $c = 2.96\,\text{Å}$, results in a strong anisotropy of the optical properties. The low-T $\epsilon_2(\omega)$ spectra along the a axis [Fig. 1(a)] are dominated by a narrow excitation at 3.93 eV (I), followed by a weaker shoulder at 4.51 eV (II) and a broader feature at 5.42 eV (III). This allows us to resolve the presence of feature II, which disappears with increasing T. In contrast, all the other excitations are clear-cut at 250 K. The c-axis spectra [Fig. 1(b)] consist instead of a single broad feature peaking at 4.15 eV (IV). The T evolution of peak energies I and III is shown in Fig. 1(c); that of peak IV, in Fig. 1(d). Remarkably, we observe a large qualitative difference in the T behavior of the excitations. Transitions I and III along the a axis display the sizable blue shift of 36 ± 6 meV with increasing T, while excitation IV along the c axis undergoes an opposite red shift of 42 ± 6 meV. To our knowledge, this is the first example of a band insulator showing opposite T behavior of the excitations along the two polarization channels. In rutile TiO_2, the thermal expansion along both axes has a regular T dependence and thus should contribute to a softening of the optical transition energies as the lattice expands with increasing T [14]. Thus, the evolution of peaks I and III with T is anomalous and is likely related to peculiar effects of the EPI at finite T.

To rationalize our data, we present *ab initio* calculations at both zero and finite T, including many-body electron-hole correlations and the effect of the EPI, as well as density-functional theory results. We first compute $\epsilon_2(\omega)$ at zero T with and without many-body electron-hole correlations. Figures 2(a) and 2(b) compare the SE data at 10 K (blue lines) with the optical spectra in the uncorrelated-particle picture (red lines) obtained within the random-phase approximation plus GW and the many-body optical spectra (violet lines)

calculated by solving the BSE (see SM for computational details [13]). As previously reported, only the inclusion of many-body correlations leads to the correct description of the experimental data [15–18]. However, already at this stage, the present combined experimental-theoretical effort has two clear advantages over previous studies: (i) the experimental $\epsilon_2(\omega)$ is measured directly via SE at 10 K, in contrast with the value extracted by a Kramers-Kronig analysis at 300 K [19], and (ii) our GW-BSE spectra are calculated with a higher degree of convergence than previously [15–18], using a fine k-point grid of $16 \times 16 \times 20$ and including 10 valence bands (VBs) and 10 conduction bands (CBs). As a consequence, we get an excellent agreement between the low-T SE spectra and the BSE calculations. Along the a axis, the sharp absorption maximum at 3.99 eV lies very close to band I (3.93 eV). A shoulder emerges around 4.57 eV, which clearly corresponds to feature II (4.51 eV). This excitation was previously not resolved either in the experimental data (obscured at 300 K) [19,20] or in the theoretical spectra (due to the lower convergence) [15–18]. Finally, a transition at 5.37 eV is also apparent, corresponding to experimental peak III (5.42 eV). Along the c axis, a doublet structure appears, whose center of mass at 4.24 eV is associated with the experimental peak IV (4.15 eV). Importantly, all these excitations lie above the direct VB-to-CB optical transition evaluated at the GW level [3.34 eV; indicated by the dashed vertical lines in Figs. 2(a) and 2(b)] and can therefore be described as resonant excitons.
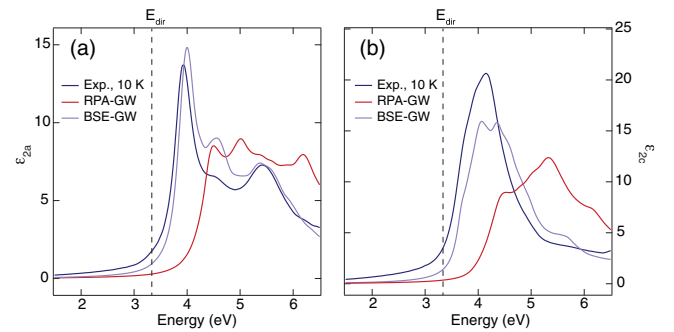

FIG. 2. Calculated imaginary part of the dielectric function at 10 K with the electric field polarized along (a) the a axis and (b) the c axis. Experimental data are represented by blue lines; spectra calculated in the random phase approximation (RPA)-GW scheme at zero T, by red lines; and spectra calculated in the BSE-GW scheme at zero T, by violet lines. The quasiparticle direct gap $E_{dir} = 3.34$ eV is indicated by the dashed vertical line.

Our calculations also find a bound exciton at 3.19 eV along both axes. However, it is optically dark and arises from transitions between the VB maximum and the CB minimum at the Γ point of the Brillouin zone. A detailed real- and reciprocal-space analysis of all the optical excitations is presented in Sec. II B of the SM [13].

We now address the observed anomalous T behavior of excitons I and III and identify its possible sources. Capturing the T dependence of the exciton peaks requires going beyond the zero T and frozen lattice approximations, including the zero-point renormalization (ZPR) as well as the effects of finite T. This becomes a formidable task, as the electrons interact with the lattice degrees of freedom in a crystal in a plethora of ways [2,21]. An assumption that is usually made involves the truncation of the electron-phonon perturbation theory series after the second-order terms [1]. Within this approximation, the most important contribution is the effect of the first-order EPI Hamiltonian to second order in perturbation theory (the so-called Fan-Migdal terms). For a simple semiconductor with parabolic and nondegenerate VBs and CBs, the Fan-Migdal matrix elements lead to the well-known "Varshni effect" [6], namely, a red shift of the band gap with increasing T (note that more complex electronic band structures might very occasionally lead to a blue shift). Depending on the details of the electron-phonon matrix element, different effects arise [21]. In the long-wavelength limit, transverse acoustic and longitudinal acoustic phonons typically couple to the electrons via the deformation potential and the piezoelectric interactions, while transverse optical (TO) and longitudinal optical (LO) modes couple via the deformation potential interaction only. An additional contribution to the first-order EPI Hamiltonian at $\mathbf{q} \sim 0$ arises in polar or partially ionic materials, since polar LO phonons can yield a macroscopic polarization, described in terms of the Fröhlich interaction [22]. Beyond Fan-Migdal terms, also the effect of second-order EPI in first-order perturbation theory (the so-called Debye-Waller or Yu-Brooks terms) has been demonstrated to provide a nonnegligible contribution [23].

A complete analysis of the EPI requires us to assess the impact of ZPR and T effects on the elementary charge excitations. As far as the ZPR is concerned, recent theoretical calculations on rutile TiO_2 estimated a decrease of 150 meV for the zero-T single-particle gap and predicted its blue shift as a function of T (in contrast to the red shift shown by other insulators) [2,24]. Unraveling the role of T is instead complicated by the presence of a higher degree of complexity compared to conventional isotropic and nonpolar materials. We first rule out any involvement of piezoelectric coupling, since rutile TiO_2 belongs to the D_{4h} space group. On the contrary, a significant contribution is expected from the deformation of the electronic potentials due to the atomic displacements. Its sign is determined by the lattice structure and the electronic states forming the VB and the CB. Its magnitude depends on the amplitude of the atomic displacement u, which in the harmonic approximation is related to the atomic effective mass μ, the eigenfrequency of the phonon mode ω, and the occupation factor n_{BE}, according to $\langle u^2 \rangle = \hbar(1 + 2n_{BE})/2\mu\omega$, where $\langle \ldots \rangle$ indicates a thermal average. The resulting shift of an exciton/interband transition energy (E_{exc}) is nearly constant at $k_B T \ll \hbar\omega$, where it is

dominated by quantum lattice fluctuations; it starts deviating around $k_B T \sim \hbar\omega$ and is proportional to T at $k_B T \gg \hbar\omega$. To account for the contribution of the deformation potential to the EPI at finite T, we calculate the single-particle (GW) and two-particle (BSE) excitation spectra when the ions in the primitive unit cell are displaced statically according to specific eigenvectors of interest. Similarly to the case of anatase, also in rutile TiO_2 the high-frequency LO $E_u^{(3)}$ mode at 829.6 cm^{-1} and the A_{2u} mode at 796.5 cm^{-1} are expected to possess the strongest coupling to the electronic degrees of freedom, at least in the a-axis response [25–27]. The eigenvectors for these modes are presented in Figs. 3(a) and 3(b). We estimate their deformation potentials to provide a possible explanation for the observed anomalous exciton blue shifts. The results of our calculations are shown in Figs. 3(c) and 3(d) along the a and the c axis, respectively. We find that (i) all excitons strongly react to a unit-cell displacement along the eigenvector of the $E_u^{(3)}$ mode from zero T to 250 K, showing the pronounced blue shift of 190 meV along the a axis and of 130 meV along the c axis (blue curves); (ii) the a-axis excitons are barely blue shifted (~ 20 meV) by a unit-cell displacement along the eigenvector of the A_{2u} mode, while peak IV shows a sizable blue shift of 60 meV (red curves). As a result, we conclude that the deformation potential interaction between the $E_u^{(3)}$ LO phonon and the in-plane charge excitations is so strong that it can account for part of the unconventional blue shift displayed by excitons I and III in the experimental spectra.

Since rutile TiO_2 is a polar material, also the Fröhlich interaction is expected to play a major role [22]. To quantify its influence on the charge excitations, we recall that the energy
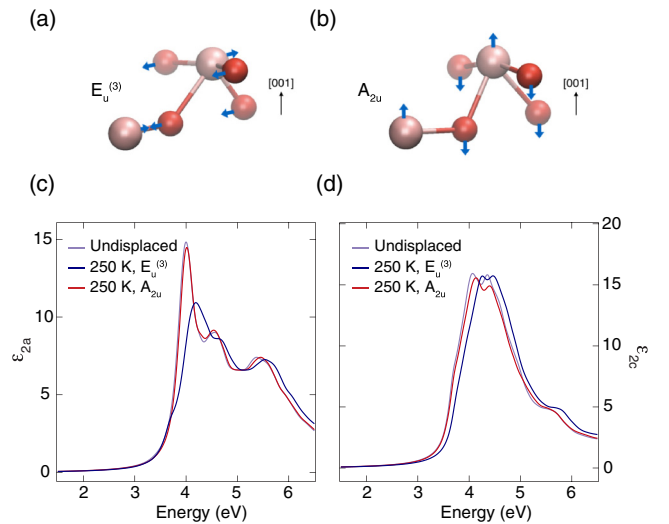

FIG. 3. Schematic of the eigenvectors for (a) the $E_u^{(3)}$ and (b) the A_{2u} phonon modes. Blue arrows indicate atomic displacements, Ti atoms are represented by pink spheres; oxygen atoms, by red spheres. (c, d) Imaginary part of the dielectric function at 10 K with the electric field polarized along (c) the a axis and (d) the c axis. Spectra calculated in the BSE-GW scheme for the undisplaced unit cell at $T = 0$ are represented by violet lines; spectra calculated for the unit cell displaced along the $E_u^{(3)}$ phonon mode at 250 K, by blue lines; and spectra calculated for the unit cell displaced along the A_{2u} phonon mode at 250 K, by red lines.

shift induced by this interaction is [22,28]

$$\Delta E_{\text{exc},\nu} = -A_\nu(\epsilon_{\infty,\nu}^{-1} - \epsilon_{0,\nu}^{-1})(1 + 2n_{\text{BE}}), \tag{2}$$

where $\nu = (a,c)$, depending on the crystal axis, and $\epsilon_{\infty,\nu}$ and $\epsilon_{0,\nu}$ are the dielectric constants at energies well above and below the phonon range, respectively. A_ν is a nearly T-independent prefactor that reads

$$A_\nu = e^2 \sum_i \sqrt{\hbar\omega_{\text{LO},i}}\,\epsilon_{\infty,\nu}\left(\frac{\sqrt{2m_e^*}}{\hbar} + \frac{\sqrt{2m_h^*}}{\hbar}\right), \tag{3}$$

where e is the fundamental charge and m_e^* (m_h^*) is the electron (hole) effective mass. The sum runs over all the i polar LO phonons at frequency ω_{LO}, which in rutile TiO_2 are represented by the $E_u^{(1)}$, $E_u^{(2)}$, $E_u^{(3)}$, and A_{2u} modes [29]. In Eqs. (2) and (3), $\epsilon_{\infty,\nu}$ and ω_{LO} are nearly T independent, while $\epsilon_{0,\nu}$ strongly varies with T. As a result, for $k_B T \ll \hbar\omega$, where n_{BE} is nearly constant, the T dependence of $\Delta E_{\text{exc},\nu}$ due to the Fröhlich interaction is determined by the T behavior of $\epsilon_{0,\nu}$. In rutile TiO_2, capacitance measurements [30] determined $\epsilon_{0,a}$ to decrease from 115 to 90 when T is raised from 4 to 300 K. Analogously, $\epsilon_{0,c}$ reduces its value from 251 to 167 for the same T increase. From our data in Figs. 1(a) and 1(b), we establish $\epsilon_{\infty,a} \sim 5.8$ and $\epsilon_{\infty,c} \sim 8$. Finally, from our *ab initio* calculations, we extract the values of m_e^* and m_h^* by performing a parabolic fit of the bands involved in the transitions contributing to excitons I and IV (see SM [13]). Substituting all values in Eq. (2) yields a blue shift of 86 meV for exciton I and of 160 meV for exciton IV.

In summary, our calculations identify that both the deformation potentials of the LO $E_u^{(3)}$ and A_{2u} normal modes and the Fröhlich interaction lead to a pronounced blue shift of all excitons in rutile TiO_2. As such, these two effects lie at the origin of the experimental shift retrieved along the a axis, albeit the latter is smaller than predicted by our calculations. This discrepancy can be related to the simultaneous contribution of other modes producing a sizable red shift, as well as to the action of the Debye-Waller terms of the EPI Hamiltonian, which are all neglected in our treatment. Moreover, we remark that Eq. (2) does not account for the presence of strong electron-hole Coulomb interaction. The latter is also expected to vary with T, since the ionic contribution to its screening (embodied by $\epsilon_{0,\nu}$) is highly T dependent. In contrast, the blue shift predicted along the c axis is not experimentally observed, and exciton IV undergoes a conventional red shift for increasing T. This implies that the Fan-Migdal terms of the EPI Hamiltonian contributing to the red shift of this exciton are much more efficient along the c axis. This behavior can depend

on the anisotropic structure of the PDOS or on the anisotropic strength of the EPI. To explain this softening, a close inspection of the partial PDOS in rutile TiO_2 is needed [29,31]. While the a-axis PDOS retains a complex structure with different modes extending between 98 and 838 cm^{-1}, the c-axis PDOS mainly shows a lower peak at 98 cm^{-1} due to transverse acoustic modes and a very prominent peak at 467 cm^{-1}. The latter is a van Hove singularity caused by the branches of the Raman-active E_g mode and the polar $E_u^{(2)}$ LO mode, and it is absent in the a-axis PDOS. As such, we expect the anisotropic deformation potential coupling to these modes to be the main cause behind the softening of exciton IV. This scenario can be confirmed phenomenologically using an approximated model based on Eq. (1), which yields an excellent and robust fit only when two Bose-Einstein oscillators, at 98 and 467 cm^{-1}, are imposed (see Sec. IV and Fig. S2 of the SM [13]). From the fit, we obtain that the high-frequency modes have a coupling ~ 5.5 larger than that of the low-frequency mode. This indicates that the effect of the LO phonons on the T dependence of exciton IV is more important than that of the transverse acoustic phonons, in accordance with the relative ratio of the peak heights ($A_{\text{LO}}/A_{\text{TO}} \sim 5.8$) in the c-axis PDOS [31]. A complete *ab initio* electron-phonon calculation, i.e., including ZPR, T effects, and electron-electron correlations, and following some of the approaches recently introduced in Refs. [24,32,33], should confirm this trend.

In conclusion, in this work we have unraveled the anisotropic evolution of the exciton peaks of rutile TiO_2 with T and reproduced the optical response of the material via many-body perturbation theory. From first-principle calculations, we evaluated different contributions of the electron-phonon coupling that lead to an anomalous blue shift/red shift of the excitonic peaks with increasing T. Our approach paves the way to a complete microscopic treatment of electron-phonon coupling and of its influence on the optical spectra of polar semiconductors, which is of pivotal importance for optimizing their applications.

---

[1] M. Cardona, Phys. Status Solidi A **188**, 1209 (2001).

[2] F. Giustino, Rev. Mod. Phys. **89**, 015003 (2017).

[3] C. Keffer, T. M. Hayes, and A. Bienenstock, Phys. Rev. Lett. **21**, 1676 (1968).

[4] P. W. Yu, W. Anderson, and Y. Park, Solid State Commu. **13**, 1883 (1973).

[5] M. Rössle, C. N. Wang, P. Marsik, M. Yazdi-Rizi, K. W. Kim, A. Dubroka, I. Marozau, C. W. Schneider, J. Humlicek, D. Baeriswyl, and C. Bernhard, Phys. Rev. B **88**, 104110 (2013).

[6] Y. P. Varshni, Physica **34**, 149 (1967).

[7] P. B. Allen and M. Cardona, Phys. Rev. B **27**, 4760 (1983).

[8] L. Vinna, S. Logothetidis, and M. Cardona, Phys. Rev. B **30**, 1979 (1984).

[9] A. T. Collins, S. C. Lawson, G. Davies, and H. Kanda, Phys. Rev. Lett. **65**, 891 (1990).

[10] M. Cardona and R. Kremer, Thin Solid Films **571**, 680 (2014).

[11] L. Hedin, Phys. Rev. **139**, A796 (1965).

[12] G. Onida, L. Reining, and A. Rubio, Rev. Mod. Phys. **74**, 601 (2002).

[13] See Supplemental Material at http://link.aps.org/supplemental/10.1103/PhysRevB.96.041204 for a description of the experimental/computational methods and for additional analysis, which includes Refs. [34–42].

[14] K. K. Rao, S. N. Naidu, and L. Iyengar, J. Am. Ceram. Soc. **53**, 124 (1970).

[15] H. M. Lawler, J. J. Rehr, F. Vila, S. D. Daloesto, E. L. Shirley, and Z. H. Levine, Phys. Rev. B **78**, 205108 (2008).

[16] L. Chiodo, J. M. Garcia-Lastra, A. Iacomino, S. Ossicini, J. Zhao, H. Petek, and A. Rubio, Phys. Rev. B **82**, 045207 (2010).

[17] W. Kang and M. S. Hybertsen, Phys. Rev. B **82**, 085203 (2010).

[18] M. Landmann, E. Rauls, and W. Schmidt, J. Phys. Condens. Matter **24**, 195503 (2012).

[19] M. Cardona and G. Harbeke, Phys. Rev. **137**, A1467 (1965).

[20] T. E. Tiwald and M. Schubert, in *International Symposium on Optical Science and Technology* (International Society for Optics and Photonics, Bellingham, WA, 2000), pp. 19–29.

[21] P. Yu and M. Cardona, *Fundamentals of Semiconductors: Physics and Materials Properties* (Springer Science & Business Media, New York, 2010).

[22] H. Fröhlich, H. Pelzer, and S. Zienau, London Edinburgh Dublin Philos. Mag. J. Sci. **41**, 221 (1949).

[23] P. B. Allen and M. Cardona, Phys. Rev. B **23**, 1495 (1981).

[24] B. Monserrat, Phys. Rev. B **93**, 100301 (2016).

[25] N. A. Deskins and M. Dupuis, Phys. Rev. B **75**, 195212 (2007).

[26] S. Moser, L. Moreschini, J. Jaćimović, O. S. Barisic, H. Berger, A. Magrez, Y. J. Chang, K. S. Kim, A. Bostwick, E. Rotenberg, L. Forró, and M. Grioni, Phys. Rev. Lett. **110**, 196403 (2013).

[27] E. Baldini, L. Chiodo, A. Dominguez, M. Palummo, S. Moser, M. Yazdi-Rizi, G. Auböck, B. P. P. Mallett, H. Berger, A. Magrez, C. Bernhard, M. Grioni, A. Rubio, and M. Chergui, Nat. Commun. **8**, 13 (2017).

[28] H. Y. Fan, Phys. Rev. **82**, 900 (1951).

[29] J. G. Traylor, H. Smith, R. Nicklow, and M. Wilkinson, Phys. Rev. B **3**, 3457 (1971).

[30] G. Samara and P. Peercy, Phys. Rev. B **7**, 1131 (1973).

[31] R. Sikora, J. Phys. Chem. Solids **66**, 1069 (2005).

[32] M. Zacharias, C. E. Patrick, and F. Giustino, Phys. Rev. Lett. **115**, 177401 (2015).

[33] M. Zacharias and F. Giustino, Phys. Rev. B **94**, 075125 (2016).

[34] D. E. Aspnes, J. Opt. Soc. Am. **70**, 1275 (1980).

[35] L. Hedin and S. Lundqvist, in *Solid State Physics*, edited by H. Ehrenreich, F. Seitz, and D. Turnbull (Academic Press, New York, 1968), Vol. 23, p. 7.

[36] J. Deslippe, G. Samsonidze, D. A. Strubbe, M. Jain, M. L. Cohen, and S. G. Louie, Comput. Phys. Commun. **183**, 1269 (2012).

[37] P. Giannozzi, S. Baroni, N. Bonini, M. Calandra, R. Car, C. Cavazzoni, D. Ceresoli, G. L. Chiarotti, M. Cococcioni, I. Dabo *et al.*, J. Phys. Condens. Matter **21**, 395502 (2009).

[38] A. M. Rappe, K. M. Rabe, E. Kaxiras, and J. D. Joannopoulos, Phys. Rev. B **41**, 1227 (1990).

[39] Y. Tezuka, S. Shin, T. Ishii, T. Ejima, S. Suzuki, and S. Sato, J. Phys. Soc. Jpn. **63**, 347 (1994).

[40] R. Lyddane, R. Sachs, and E. Teller, Phys. Rev. **59**, 673 (1941).

[41] M. H. Manghnani, J. Geophys. Res. **74**, 4317 (1969).

[42] W.-J. Yin, S. Chen, J.-H. Yang, X.-G. Gong, Y. Yan, and S.-H. Wei, Appl. Phys. Lett. **96**, 221901 (2010).